

# Enhancement of polar phase of PVDF by forming PVDF/SiC nanowire composite

Jie-Fang Huang, Song-Jia Han, Hui-Jiuan Chen, Gui-Shi Liu, Gong-Tan Li, Yu-Cheng Wang, Zi-Xin Wang\*, Bo-Ru Yang\*

The State Key Laboratory of Optoelectronic Materials and Technologies, School of Electronics and Information Technology, and SYSU-CMU Shunde International Joint Research Institute, Sun Yat-Sen University, Guangzhou, 510006, China

\*E-mail: wangzix@mail.sysu.edu.cn, paulyang68@icloud.com

Zhen-Hua Luo

School of Water, Energy and Environment, Cranfield University, Cranfield, Bedfordshire, MK43 0AL, UK

and Han-Ping D. Shieh

The Department of Photonics and Display Institute, National Chiao Tung University, Hsinchu, 300, Taiwan

## ABSTRACT

**Different contents of silicon carbide (SiC) nanowires were mixed with Poly(vinylidene fluoride) (PVDF) to facilitate the polar phase crystallization. It was shown that the annealing temperature and SiC content affected the phase and crystalline structures of PVDF/SiC samples. Furthermore, the addition of SiC nanowire enhanced the transformation of non-polar  $\alpha$  phase to polar phases and increased the relative fraction of  $\beta$  phase in PVDF. Due to the nucleating agent mechanism of SiC nanowires, the interfacial interaction between the negatively charged surface of SiC nanowires and the positively charged  $\text{CH}_2$  groups of PVDF facilitated the formation of polar phases in PVDF.**

**Index Terms — Poly(vinylidene fluoride); silicon carbide nanowires; polar phase; annealing temperature; content.**

## 1 INTRODUCTION

PIEZOELECTRIC materials are commonly used for pressure sensing [1-2], energy harvesting [3], health monitoring [4-5], etc. Comparing to piezoelectric crystals and piezoelectric ceramics, piezoelectric polymers are considered as the ideal materials for wearable pressure sensor devices, owing to their high dielectric constant, flexibility, and biocompatibility. Among all the piezoelectric polymers, Polyvinylidene fluoride (PVDF) is one of the most investigated materials. The structure of PVDF molecules is a macromolecular chain, which consists of repeated units of  $\text{CH}_2$  groups and  $\text{CF}_2$  groups. It is a semi-crystalline polymershowing complex polycrystalline structures and can be divided into five crystalline phases:  $\alpha$ ,  $\beta$ ,  $\gamma$ ,  $\delta$ , and  $\epsilon$  phases, which are related to different chain conformations [6-7]. The  $\alpha$  phase is the most common crystalline phase and its main chain conformation presents as TGTG' (trans-gauche-trans-gauche) structure. The dipole moments of  $\alpha$ -PVDF are reversely arranged in order, showing no piezoelectricity. The PVDF film fabricated by slowly cooling from melt or solution casting will mostly contributes to  $\alpha$  phase [8-9]. The  $\alpha$  phase of PVDF can transform into  $\delta$  phase by poling the material in strong electric

field to obtain feeble piezoelectricity. In the  $\beta$  phase of PVDF, the polymer chains have the all-*trans* (TTTT) planar zigzag conformation, in which hydrogen atoms and fluorine atoms are arranged on the opposite sides of the main chain, respectively. As for the  $\beta$  phase of PVDF, dipole moments point in the same direction, showing the strongest piezoelectricity. The  $\gamma$  phase of PVDF is formed from melting crystallization at high temperature (about 170°C) [10]. The  $\gamma$  and  $\epsilon$  phases, with the main chain conformation of  $\text{T}_3\text{GT}_3\text{G}'$ , have weaker piezoelectricity in comparison with  $\beta$  phase, due to the T-G bond which presents at every third repeated T-T bond. Among these five phases, the non-polar  $\alpha$  phase and the polar phases ( $\beta$  and  $\gamma$  phases) of PVDF are the most investigated.

Many treatments have effects on the crystalline structures of PVDF, including mechanical stretching [11], heat treatment [12], electric field poling [13], electrospinning [14], [15], solvents species [16]. In recent years, some research works indicate that mixing PVDF with nano-fillers facilitates the formation of  $\beta$  phase in PVDF and improves its piezoelectricity. Indolia and Gaur added various contents of ZnO nanoparticles into PVDF solution to investigate the structural characteristics of PVDF/ZnO [17]. The degree of  $\beta$  phase increased when higher ZnO nanoparticle contents were

mixed in the PVDF film. Thakur *et al.* found that the addition of kadinite and halloysite induced the transformation of  $\alpha$  phase into  $\beta$  phase [18]. According to the nucleation mechanism, the interaction between the kadinite/halloysite and the groups of PVDF can enhance the  $\beta$  phase crystallinity. Ye *et al.* incorporated PVDF films with tetradecylphosphonic acid (TDPA)-BaTiO<sub>3</sub> [19]. They obtained a high crystallinity of  $\beta$  phase PVDF at about 93% with a TDPA-BaTiO<sub>3</sub> nanoparticles content of 20%. Other kinds of nano-fillers such as ferrite nanoparticles [20], gold nanoparticles [21], TiO<sub>2</sub> nanoparticles [22], clays [23] have been mixed into PVDF to enhance the piezoelectricity of PVDF film. As a ceramic and semiconductor material, silicon carbide (SiC) exhibits stable chemical properties, high thermal conductivity, small thermal expansion coefficient, and good wear resistance [24]. Mixing ceramic materials with PVDF is a simple way to improve the properties of the polymer [25]. SiC nanoparticle provides much larger length-to-diameter and surface-to-volume ratios than SiC nanowire and bulk SiC. Although some works have previously investigated the PVDF/SiC nanoparticles, mixing PVDF with SiC nanowires has not been comprehensively investigated and its mechanism is still not fully understood.

In this work, we utilize SiC nanowires as a nucleating agent to facilitate the transformation of  $\alpha$  phase into polar phases, improving the relative fraction of  $\beta$  phase in PVDF thin film. Thin films were prepared by solution processing at different ratios of PVDF/SiC. We investigated the crystalline structures and surface morphology of pure PVDF and PVDF/SiC nanowire composites, which were annealed at different temperatures. The interaction mechanism between PVDF and SiC nanowires was investigated and explained.

## 2 EXPERIMENTAL

### 2.1 MATERIALS

PVDF (M<sub>w</sub>=534,000) and N,N-dimethylacetamide (DMAc, purity of 99%) were purchased from Sigma Aldrich (St. Louis, Mo, USA). SiC nanowires (diameter of 100-600 nm, length of about 100  $\mu$ m, purity of 98%) were purchased from Xianfeng Nanomaterial Inc (Nanjing, China).

### 2.2 PROCESSING

PVDF powder was dissolved in N,N-dimethylacetamide (DMAc) solvent at the content of 10 wt% and stirred at room temperature on the magnetic stirrer for four hours until PVDF was completely dissolved. Different weights of SiC nanowires were added into PVDF solvent at the contents of 0 wt%, 2 wt%, 5 wt%, and 8 wt%, respectively. By stirring at room temperature for over 48 hours and ultra-sonicating for one hour, good dispersion of SiC in PVDF solution was achieved. The solution of PVDF/SiC was drop-casted on a dry glass, which was cleaned in acetone, alcohol, and de-ionized water for 15 minutes, respectively. The pure PVDF and PVDF/SiC composite samples were annealed on a hot plate at 140°C and 80°C for 2 hours, respectively, to evaporate DMAc solvent completely, then cooled slowly at the rate of about 1°C/min to

room temperature. Pure PVDF and PVDF/SiC composites were crystallized during these annealing processes. The sample films after cooling were peeled off and prepared for the following testing and characterization.

## 2.3 CHARACTERIZATION

In order to identify the polycrystalline structures of pure PVDF and PVDF/SiC composites with different SiC contents and annealed at different temperatures, optical microscope (OM, AxioCam MRC 5, ZEISS), scanning electron microscope (SEM, Carl Zeiss Microscopy GmbH, SUPRA 60) and atomic force microscope (AFM, NTEGRA Spectra) were used to observe the surface morphology. X-ray diffraction (XRD, Empyrean) and fourier transform infrared spectroscopy (FT-IR, EQUINOX 55) were used to analyze the crystalline structures of pure PVDF and PVDF/SiC composite films. Differential scanning calorimetry (DSC, Netzsch 204) was used to measure the overall crystallinity of the PVDF samples. Stylus profiler (Veeco Dektak 150) was used to measure the thickness of the PVDF/SiC films. Energy dispersive spectroscopy (EDS, X-Max<sup>N</sup>, Oxford Instrument) was used to detect the chemical element contents in SiC nanowires, and a multi-parameter tester (S470-USP/EP SevenExcellence<sup>TM</sup> pH/Conductivity Meter Kit, Mettler Toledo) was used to measure the acid-base property of DMAc solvent.

## 3 RESULTS

### 3.1 CRYSTALLINE STRUCTURES AND SURFACE MORPHOLOGY OF PURE PVDF ANNEALED AT 140°C AND 80°C

Annealing temperature has influence on the crystalline phase of PVDF. Figure 1 shows the XRD patterns of pure PVDF annealed at 140°C and 80°C. When the pure PVDF film was annealed at 140°C, the crystalline phase of pure PVDF was mainly  $\alpha$  phase. The diffraction peaks at 17.7°, 18.3°, 19.9°, and 26.6° correspond to the  $\alpha$  phase at the (100), (020), (110), and (021) planes of the  $\alpha$  phase of PVDF, respectively [26-27]. When the pure PVDF was annealed at 80°C, the  $\beta$  phase of PVDF with the diffraction peak of 20.3° and  $\gamma$  phase of PVDF with the diffraction peak of 18.7° were observed in the XRD pattern [26]. From the FT-IR spectra shown in Figure 1b, the characteristic bands at 1180 and 880 cm<sup>-1</sup> are assigned to the vibration of carbon-carbon skeleton, 1402 cm<sup>-1</sup> corresponds to the swing vibration of CH<sub>2</sub>, and 1170 cm<sup>-1</sup> is related to the stretching vibration of CF<sub>2</sub> [28-29]. The characteristic bands at 764, 795, 855, 976, 1147, 1210, and 1383 cm<sup>-1</sup> correspond to  $\alpha$  phase of PVDF [26-27, 30]. Although a weak characteristic band of 840 cm<sup>-1</sup> presented in the pure PVDF treated at 140°C, most of the characteristic bands were related to  $\alpha$  phase. This coincided with the XRD result. It confirmed that the domain crystalline form of pure PVDF annealed at 140°C was  $\alpha$  phase. Whereas at 80°C, the absorption band of  $\beta$  phase at 840 cm<sup>-1</sup> and absorption band of  $\gamma$  phase at 1234 cm<sup>-1</sup> were clearly observed [26-27]. In the

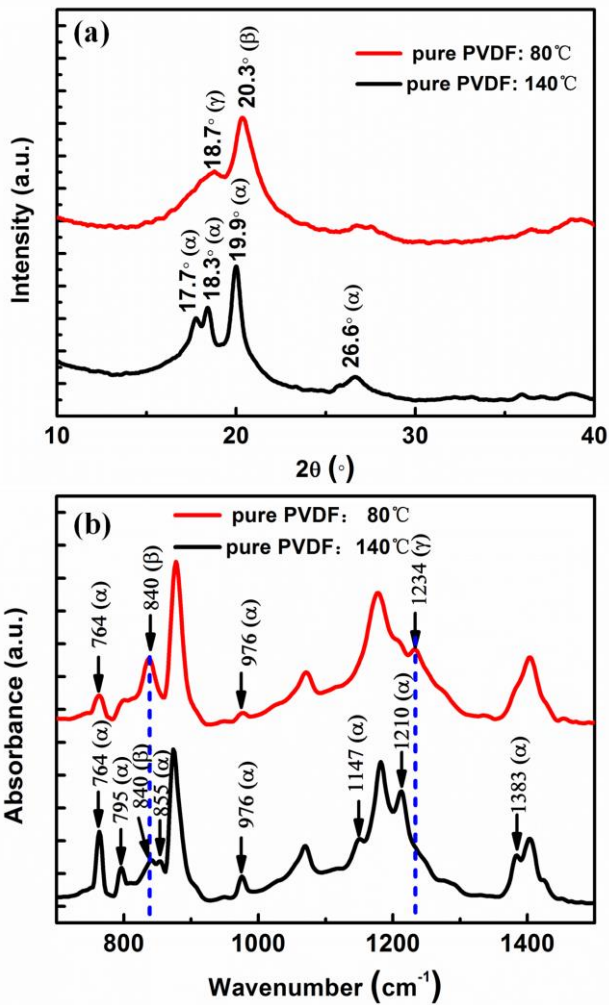


Figure 1. (a) XRD patterns and (b) FT-IR spectra of pure PVDF annealed at 140°C and 80°C

meantime, the intensity of all the characteristic bands corresponding to  $\alpha$  phase was less or even not observed. This showed that the dominant crystalline structure were  $\beta$  and  $\gamma$  phases instead of  $\alpha$  phase. Both XRD patterns and FT-IR spectra proved that the annealing temperature has influence on the crystalline phases of PVDF. When the annealing temperature was around 140°C, PVDF was inclined to form non-polar  $\alpha$  phase instead of polar  $\beta$  phase. This coincides with the explanation from Hsu and Geil [31].

### 3.2 SURFACE MORPHOLOGY OF PURE PVDF ANNEALED AT 140°C AND 80°C

The  $\alpha$  and  $\beta$  phases of PVDF show different surface morphologies. The SEM and AFM topographic images of pure PVDF further provided evidence of phase transformation between the annealing temperature of 140°C and 80°C. Before the observation of SEM, a thin layer of fine gold was deposited on the surface of the samples to avoid accumulating negative charges. From Figure 2, we observed that the crystalline morphology of PVDF annealed at 140°C mostly exhibited the

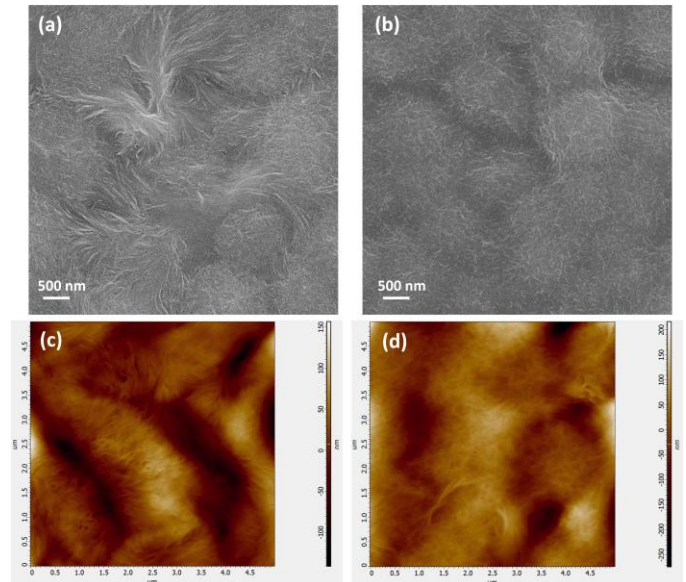


Figure 2. SEM images of pure PVDF annealed at (a) 140°C and (b) 80°C; AFM topographic images of pure PVDF annealed at (c) 140°C and (d) 80°C.

large isotropic spherulite structure, which indicated the dominant crystalline phase was  $\alpha$  phase [25, 32]. The surface of PVDF annealed at 80°C were mostly covered with the crystallite structure which was related to  $\beta$  phase [32]. Furthermore, the AFM topographic image of pure PVDF annealed at 140°C exhibited long and thick wool-like structures, whereas the pure PVDF annealed at 80°C mostly showed fine fiber-like surface. The AFM result indicated that the PVDF sample annealed at 140°C has a lower surface roughness ( $R_q=36.6$  nm), whereas the PVDF sample annealed at 80°C has a rougher surface ( $R_q=67.9$  nm). [The surface roughness of the film was analyzed to quantify the following parameters: RMS ( $R_q$ ).] Both of the SEM and AFM topographic images revealed that pure PVDF was inclined to form  $\alpha$  phase when annealed at 140°C, and to form  $\beta$  phase at 80°C.

### 3.3 CRYSTALLINE STRUCTURE OF PVDF/SiC COMPOSITES ANNEALED AT 140°C AND 80°C

To investigate the effect of SiC nanowires on the crystalline structure of PVDF, various contents of SiC nanowires were added into PVDF solution. The SiC nanowires were found to be well dispersed in the PVDF matrix as indicated by SEM image (Figure 3a). The morphology of SiC nanowire was clearly observed at higher magnification of SEM image (Figure 3b). The diameter of the nanowire was about 500 nm. The optical microscope image showed the various lengths of SiC nanowires (Figure 3c). The thickness of PVDF/SiC film was about 25~30  $\mu\text{m}$  as measured by stylus profiler.

In the FT-IR spectra of pure PVDF and PVDF/SiC composites shown in Figure 4, the absorption band presented at 802  $\text{cm}^{-1}$  is assigned to the stretching vibration peak of Si-C bond [33].



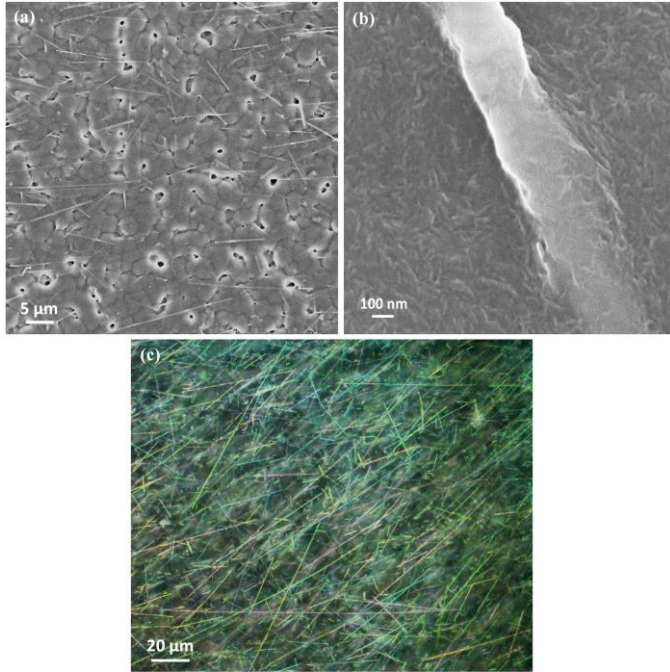


Figure 3. (a) Low magnified image of SEM shows SiC nanowires were well dispersed in the PVDF matrix; (b) High magnified image of SEM presents the diameter of SiC nanowires; (c) The image of optical microscope present the length of SiC nanowires.

When pure PVDF annealed at the temperature of 140 °C, the dominant crystalline form was  $\alpha$  phase. However, with the addition of SiC nanowires, the characteristic bands of  $\alpha$  phase significantly decreased and even disappeared at higher doping concentrations, as shown in Figure 4a. At the close overlapping of the characteristic band of Si-C bond located at 802 cm<sup>-1</sup> and the  $\alpha$  phase located at 795 cm<sup>-1</sup> in the spectra, the growing of absorption band at approximately 800 cm<sup>-1</sup> is ascribed to the Si-C bond with the increasing ratio of PVDF/SiC. In the meantime, the characteristic band of 840 cm<sup>-1</sup> corresponding to the  $\beta$  phase and the characteristic band of 1234 cm<sup>-1</sup> corresponding to the  $\gamma$  phase were enhanced distinctly. As for the PVDF samples annealed at 80 °C,  $\beta$  phase was the domain crystalline phase of pure PVDF. After mixing with SiC nanowires, the characteristic band of  $\gamma$  phases was enhanced, whereas the characteristic band of  $\beta$  phase was almost intact (Figure 4 and their partial enlarged drawings at the upper right corner). However, the characteristic bands of  $\alpha$  phase located at 764, 976, and 1210 cm<sup>-1</sup> were almost disappeared completely. Therefore, the results of FT-IR spectra confirmed that SiC nanowires promoted the formation of polar phases of PVDF while depressing the formation of  $\alpha$  phase.

### 3.4 OVERALL CRYSTALLINITY AND PHASE CONTENT OF PURE PVDF AND PVDF/SiC COMPOSITES

As one of the two most common crystalline structures (non-polar  $\alpha$  phase and polar  $\beta$  phase) of PVDF, the  $\beta$  phase is of great importance in the applications of PVDF because of its

pyro- and piezoelectric properties [34]. Therefore, increasing the

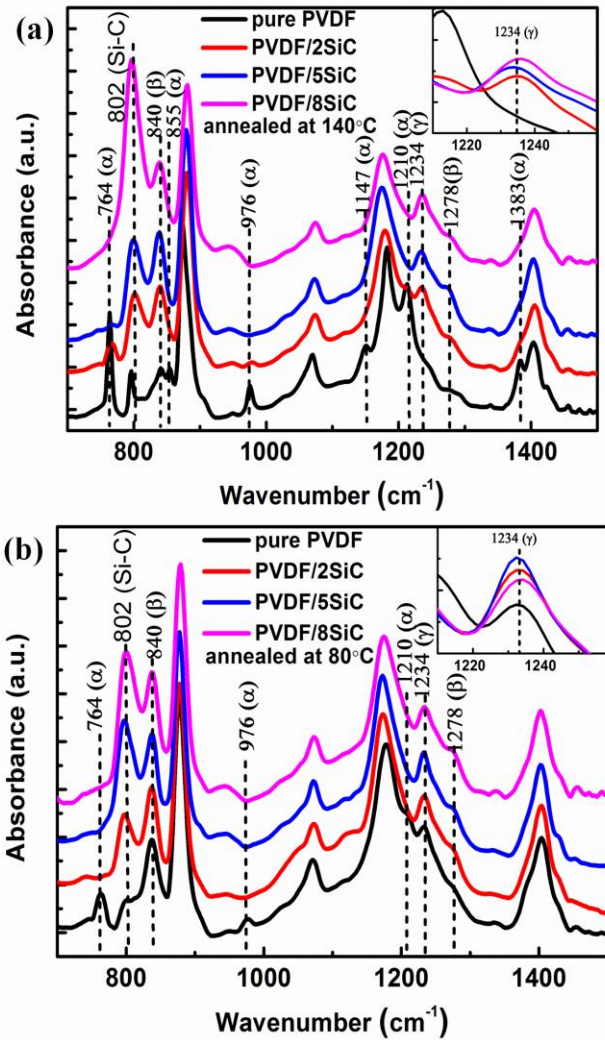


Figure 4. FT-IR spectra of pure PVDF and PVDF/SiC composites annealed at (a) 140 °C and (b) 80 °C

relative fraction of  $\beta$  phase is the key in improving the performances of PVDF polymer.

The overall crystallinity of the polymer can be obtained from the DSC thermograms. The samples were melted at 200 °C for 10 min to erase the thermal history, then cooled from 200 to 20 °C at a rate of 10 °C/min, and heated from 20 °C to 200 °C at the same rate. The DSC measurement processing was performed in N<sub>2</sub> atmosphere. The overall crystallinity of pure PVDF and PVDF/SiC composite can be calculated using the following equation:

$$X_c(\%) = \frac{\Delta H_m}{\Delta H_0} \quad (1)$$

where  $\Delta H_m$  is the actual melting enthalpy of the sample,  $\Delta H_0$  is the melting enthalpy of 100% crystalline sample. The melting enthalpy of 100% crystalline PVDF is 104.6 J/g [35]. The DSC results of pure PVDF and PVDF/SiC composite were shown in Table 1. As shown in Table 1, the overall crystallinity in PVDF/SiC composites is less than the pure

PVDF. This is due to the fact that in the process of transforming  $\alpha$  phase into  $\beta$  phase, the reduction in  $\alpha$  phase crystallinity was more than the increase of  $\beta$  phase crystallinity. This is clearly seen in the FT-IR spectra. The maximum  $X_c$  was found to be 53.4% for pure PVDF sample, whose domain crystal was  $\alpha$  phase. For the PVDF/SiC composites, the overall crystallinity  $X_c$  increased with the increasing content of SiC nanowires. However, further measurement will need be taken for calculating the relative fraction of  $\beta$  phase in the pure PVDF and PVDF/SiC composites.

**Table 1. Overall Crystallinity of pure PVDF and PVDF/SiC composites**

| Samples   | $\Delta H_m$ (J/g) | $X_c$ (%) |
|-----------|--------------------|-----------|
| PVDF      | 53.6               | 53.4      |
| PVDF/2SiC | 46.0               | 45.8      |
| PVDF/5SiC | 48.8               | 48.6      |
| PVDF/8SiC | 49.2               | 49.0      |

FT-IR spectra are commonly used to calculate the relative fraction of  $\beta$  phase by quantifying the  $\alpha$  and  $\beta$  phases of PVDF at the characteristic absorption bands of 764 and 840  $\text{cm}^{-1}$ , which was explained by Gregorio [11-12, 19]. This method is based on the assumption that FT-IR absorption obeys the Lambert-Beer law, and it was used in multiple studies [11, 18, 23]. The absorption coefficients  $K_\alpha$  and  $K_\beta$  are calculated at the absorption bands of 764 and 840  $\text{cm}^{-1}$ . The relative fraction of  $\beta$  phase in PVDF samples containing  $\alpha$  and  $\beta$  phases can be calculated using the following equation [12]:

$$F(\beta) = \frac{X_\beta}{X_\alpha + X_\beta} = \frac{A_\beta}{\left(\frac{K_\beta}{K_\alpha}\right)A_\alpha + A_\beta} = \frac{A_\beta}{1.26A_\alpha + A_\beta} \quad (2)$$

Where  $F(\beta)$  is the relative  $\beta$  phase content of the sample;  $A_\alpha$  and  $A_\beta$  represent the absorbance at the bands of 764 and 840  $\text{cm}^{-1}$ ;  $K_\alpha$  and  $K_\beta$  are the absorption coefficients at the corresponding wavenumber. The values of  $K_\alpha$  and  $K_\beta$  are  $6.1 \times 10^4$  and  $7.7 \times 10^4$   $\text{cm}^2/\text{mol}$ , respectively [12].

For the PVDF/SiC composites, the variation of the relative  $\beta$  phase fraction as a function of the increasing content of SiC nanowires was shown in Figure 5. Generally, the relative fraction of  $\beta$  phase firstly increases upon increasing the doping concentration of SiC nanowires, and then reaches a maximum value at certain concentration of SiC nanowires. This pattern was observed in both cases where the samples were annealed at 140  $^\circ\text{C}$  and 80  $^\circ\text{C}$ , but showing different curve growing profiles and different optimized doping concentrations. For PVDF annealed at 140  $^\circ\text{C}$ , the relative crystalline fraction of  $\beta$  phase was only 17%. With the addition of SiC nanowires, the relative fraction of  $\beta$  phase increased markedly and reached a maximum value of around 54% at the doping concentration of 5 wt%. PVDF/SiC composite samples annealed at 80  $^\circ\text{C}$  presented higher relative fractions of  $\beta$  phase than those annealed at 140  $^\circ\text{C}$  at the same doping SiC nanowire concentration. A maximum  $\beta$  phase fraction of around 80% was seen in the sample with 2 wt% SiC nanowire concentration and annealed at 80  $^\circ\text{C}$ . After the maximum value was reached, the relative fraction of  $\beta$  phase began to reduce as

the SiC doping concentration increased further, which coincided

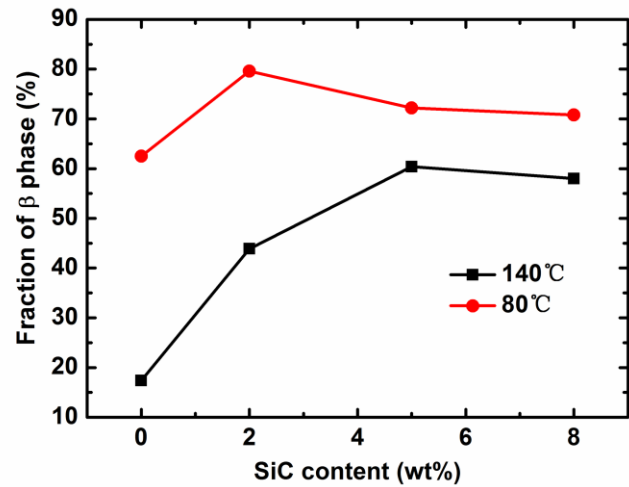
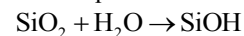


Figure 5. Relative fraction of  $\beta$  phase with increasing SiC nanowires content.

with the results of PVDF/kaolinite and PVDF/TDPA-BaTiO<sub>3</sub> obtained by Thakur and Ye, respectively [18-19]. Obviously, mixing PVDF with SiC nanowires can improve the relative fraction of  $\beta$  phase in the PVDF/SiC composites, especially at the annealing temperature of 80  $^\circ\text{C}$ . Even for the pure PVDF that form little  $\beta$  phase when annealed at 140  $^\circ\text{C}$ , adding certain value of SiC nanowires can substantially increase the relative fraction of  $\beta$  phase.

## 4 DISCUSSION

FT-IR spectra indicates that the addition of SiC nanowires favors the formation of polar phases in PVDF. It is conceived that SiC nanowires can interact with PVDF molecules, facilitating the formation of polar phases and reducing the proportion of non-polar  $\alpha$  phase. In order to explore the interacting mechanism between PVDF polymer and SiC nanowires, we investigated the surface of SiC nanowires. The surface of SiC nanowires can be easily oxidized and form a thin (1-2 nm) amorphous film which is mostly SiO<sub>2</sub> [36]. To prove the existence of SiO<sub>2</sub> in the SiC nanowires, energy dispersive spectroscopy (EDS) tests were conducted to measure the chemical contents of the nanowires. In the EDS spectra of the raw SiC nanowires, the chemical element of carbon, oxygen, and silicon were detected with the weight percentage values of 15.38%, 0.78%, and 83.84%, respectively. It indicated that the surface of the SiC nanowires was oxidized and a thin SiO<sub>2</sub> layer was formed. When SiC nanowires were dispersed in the reaction solution, the amorphous SiO<sub>2</sub> thin films (Si-O-Si bond) on the surface of SiC nanowire will hydrolyze and form the stable silanol (Si-OH) films. The process of SiO<sub>2</sub> hydrolysis reaction can be described by the chemical equation shown below:



SiOH will generate positively charged  $[\text{SiOH}_2]^+$  in acidic conditions and create negatively charged  $\text{SiO}^-$  and water by dehydrogenation in alkaline environment, as following shown

[37]:

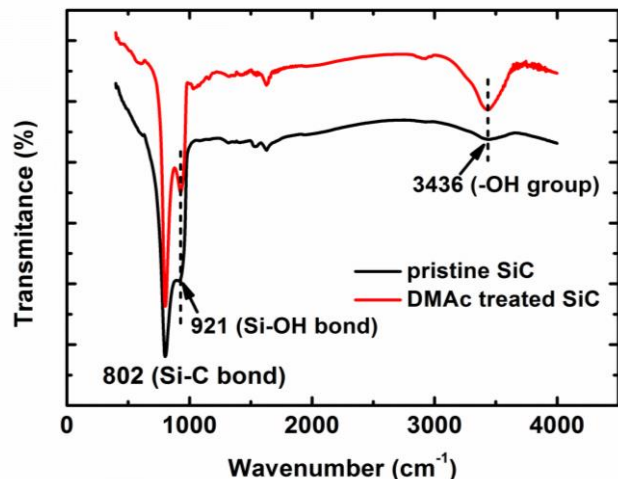
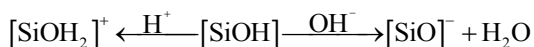


Figure 6. FT-IR spectra of pristine SiC nanowires and SiC nanowires treated with DMAC solution.



The pH value of DMAC solvent used in the treatment solution was measured by the multi-parameter tester and its value was 10.11, which indicated that DMAC solution was alkaline. As shown in the FT-IR spectra of pristine SiC nanowires and SiC nanowires treated with DMAC (Figure 6), the characteristic bands at 921  $\text{cm}^{-1}$  (Si-OH stretching) and 3436  $\text{cm}^{-1}$  (-OH group) were enhanced, indicating that DMAC could facilitate the hydrolysis of  $\text{SiO}_2$  and form more Si-OH bonds on the surface of SiC nanowire [38]. In alkaline conditions, the Si-OH groups will transfer the proton ( $\text{H}^+$ ) to the basic species in the solvent, forming the anionic group Si-O $^-$  on the SiC nanowire surface [37], as shown in Figure 7b. Therefore, the surface of SiC nanowire was negatively charged. The negatively charged surface of SiC nanowires and the positive charge of  $\text{CH}_2$  groups of PVDF exhibited an affinity between

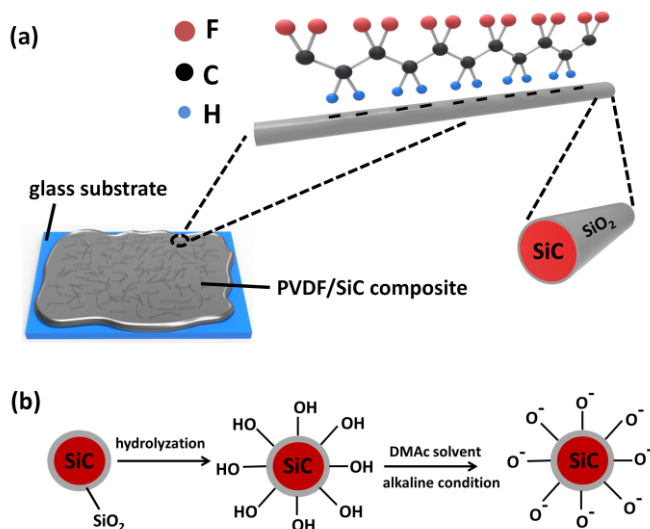


Figure 7. (a) Schematic representation of the interaction mechanism between PVDF polymer and SiC nanowires; (b) The flow chart of chemical reactions

occur on the surface of SiC nanowire.

the SiC nanowires and PVDF. The ion-dipole interaction caused the polymer chains to align on the SiC nanowire surface, facilitating the preferential formation of  $\beta$  and  $\gamma$  phases chain conformation of PVDF, as shown in Figure 7a. The enhancement of  $\beta$  phase crystallization of PVDF was attributed to the regular dipole orientation and PVDF molecular chain alignment along SiC nanowires in long-range order. Therefore, SiC nanowires acted as the nucleating agents and favored the formation of all-*trans* planar zigzag chain conformation of PVDF. Similar mechanisms were reported in the previous studies: the formation of  $\beta$ -PVDF with modified clay [23], kaolinite/halloysit [18], palladium nanoparticles [32], gold nanoparticle and gold nanoshell [39]. Due to the different extents of interaction force between the  $\text{CH}_2$  groups and negatively charged surface of SiC nanowires upon their distance, PVDF polymer may form  $\beta$  phase in the vicinity of SiC nanowire, and form  $\gamma$  phase with a slight distance away from the SiC nanowire.

## 5 CONCLUSION

In this work, pure PVDF and PVDF/SiC-nanowire composite films with different SiC doping concentrations of 2 wt%, 5 wt%, and 8 wt% were prepared by solution processing. The samples were annealed at 140 $^\circ\text{C}$  and 80 $^\circ\text{C}$ , respectively, to investigate the phase and crystalline structures transformations of PVDF. Annealing temperature and SiC doping concentrations have significant effects on the phase types and phase fractions. The maximum relative fraction of  $\beta$  phase in PVDF of about 54% was obtained at the doping SiC nanowire concentration of 5 wt% when the annealing temperature was 140 $^\circ\text{C}$ . As for the samples annealed at 80 $^\circ\text{C}$ , the  $\beta$  phase presented higher fraction of about 80% at the SiC nanowire concentration of 2 wt%. The electrostatic interaction between the  $\text{CH}_2$  dipoles of PVDF and negatively charged surface of SiC nanowires led to the change in dipole orientation. As a result, the molecular chains of PVDF orderly aligned along the SiC nanowires and the  $\text{CF}_2$  dipoles arranged in the direction perpendicular to the polymer chain, which favored the formation of polar phases, and could potentially improve the piezoelectric property of PVDF polymer.

## ACKNOWLEDGMENT

This work was financially supported by the projects from the National High Technology Research and Development Program of China (863 Project) (2015AA033408), the National Natural Science Foundation of China (61307027), the Science and Technology Program of Guangdong Province (2014-B090914001), and Shunde Government, Guangdong Province, China (20140401).



## REFERENCES

- [1] A. Kimoto, N. Sugitani, and S. Fujisaki, "A Multifunctional Tactile Sensor Based on PVDF Films for Identification of Materials," *IEEE Sens. J.*, Vol. 10, No. 9, pp. 1508-1513, Sep, 2010.
- [2] T. Sharma, S. Naik, J. Langevine, B. Gill, and J. X. J. Zhang, "Aligned PVDF-TrFE Nanofibers With High-Density PVDF Nanofibers and PVDF Core-Shell Structures for Endovascular Pressure Sensing," *IEEE T. Bio-med Eng.*, Vol. 62, No. 1, pp. 188-195, Jan, 2015.
- [3] V. Bhavanasi, V. Kumar, K. Parida, J. X. Wang, and P. S. Lee, "Enhanced Piezoelectric Energy Harvesting Performance of Flexible PVDF-TrFE Bilayer Films with Graphene Oxide," *ACS Appl. Mater. Inter.*, Vol. 8, No. 1, pp. 521-529, Jan 13, 2016.
- [4] B. Y. Ren, and C. J. Lissenden, "PVDF Multielement Lamb Wave Sensor for Structural Health Monitoring," *IEEE T. Ultrason. Ferr.*, Vol. 63, No. 1, pp. 178-185, Jan, 2016.
- [5] D. H. Wang, and S. L. Huang, "Health monitoring and diagnosis for flexible structures with PVDF piezoelectric film sensor array," *J. of Intell. Mat. Sys. Str.*, Vol. 11, No. 6, pp. 482-491, Jun, 2000.
- [6] A. J. Lovinger, "Annealing of poly(vinylidene fluoride) and formation of a fifth phase," *Macromolecules*, Vol. 15, No. 1, pp. 40-44, 1982.
- [7] M. Benz, and W. B. Euler, "Determination of the crystalline phases of poly(vinylidene fluoride) under different preparation conditions using differential scanning calorimetry and infrared spectroscopy," *J. Appl. Polym. Sci.*, Vol. 89, No. 4, pp. 1093-1100, Jul 25, 2003.
- [8] K. Sakaoku, and A. Peterlin, "Poly(vinylidene fluoride) single crystals," *J. of Macromol. Sci. B*, Vol. 1, No. 2, pp. 401-406, 1967.
- [9] K. Okuda, T. Yoshida, M. Sugita, and M. Asahina, "Solution-grown crystals of poly(vinylidene fluoride)," *J. Polym. Sci. Polym. Lett.*, Vol. 5, No. 6, pp. 465-468, 1967.
- [10] P. Martins, A. C. Lopes, and S. Lanceros-Mendez, "Electroactive phases of poly(vinylidene fluoride): Determination, processing and applications," *Progr. Polym. Sci.*, Vol. 39, No. 4, pp. 683-706, Apr, 2014.
- [11] J. Gomes, J. Serrado Nunes, V. Sencadas, and S. Lanceros-Mendez, "Influence of the  $\beta$ -phase content and degree of crystallinity on the piezo- and ferroelectric properties of poly(vinylidene fluoride)," *Smart Mater. Struct.*, Vol. 19, No. 6, pp. 065010, 2010.
- [12] J. R. Gregorio, and M. Cestari, "Effect of crystallization temperature on the crystalline phase content and morphology of poly(vinylidene fluoride)," *J. Polym. Sci. Pol. Phys.*, Vol. 32, No. 5, pp. 859-870, 1994.
- [13] G. T. Davis, J. E. McKinney, M. G. Broadhurst, and S. C. Roth, "Electric-field-induced phase changes in poly(vinylidene fluoride)," *J. Appl. Phys.*, Vol. 49, No. 10, pp. 4998, 1978.
- [14] J. F. Zheng, A. H. He, J. X. Li, and C. C. Han, "Polymorphism control of poly(vinylidene fluoride) through electrospinning," *Macromol. Rapid Comm.*, Vol. 28, No. 22, pp. 2159-2162, Nov 16, 2007.
- [15] G. Y. Ren, F. Y. Cai, B. Z. Li, J. M. Zheng, and C. Y. Xu, "Flexible Pressure Sensor Based on a Poly(VDF-TrFE) Nanofiber Web," *Macromol. Mater. and Eng.*, Vol. 298, No. 5, pp. 541-546, May, 2013.
- [16] A. Salimi, and A. A. Yousefi, "Conformational changes and phase transformation mechanisms in PVDF solution-cast films," *J. Polym. Sci. Pol. Phys.*, Vol. 42, No. 18, pp. 3487-3495, 2004.
- [17] A. P. Indolia, and M. S. Gaur, "Investigation of structural and thermal characteristics of PVDF/ZnO nanocomposites," *J. Therm. Anal. Calorim.*, Vol. 113, No. 2, pp. 821-830, 2012.
- [18] P. Thakur, A. Kool, B. Bagchi, S. Das, and P. Nandy, "Enhancement of beta phase crystallization and dielectric behavior of kaolinite/halloysite modified poly(vinylidene fluoride) thin films," *Appl. Clay Sci.*, Vol. 99, pp. 149-159, Sep, 2014.
- [19] H. J. Ye, W. Z. Shao, and L. Zhen, "Crystallization kinetics and phase transformation of poly(vinylidene fluoride) films incorporated with functionalized baTiO<sub>3</sub> nanoparticles," *J. Appl. Polym. Sci.*, Vol. 129, No. 5, pp. 2940-2949, Sep 5, 2013.
- [20] P. Martins, X. Moya, L. C. Phillips, S. Kar-Narayan, N. D. Mathur, and S. Lanceros-Mendez, "Linear anhysteretic direct magnetoelectric effect in Ni<sub>0.5</sub>Zn<sub>0.5</sub>Fe<sub>2</sub>O<sub>4</sub>/poly(vinylidene fluoride-trifluoroethylene) 0-3 nanocomposites," *J. Phys. D Appl. Phys.*, Vol. 44, No. 48, pp. 482001, 2011.
- [21] W. Wang, S. Zhang, L.-o. Srisombat, T. R. Lee, and R. C. Advincula, "Gold-Nanoparticle- and Gold-Nanoshell-Induced Polymorphism in Poly(vinylidene fluoride)," *Macromol. Mater. Eng.*, Vol. 296, No. 2, pp. 178-184, 2011.
- [22] N. L. An, H. Z. Liu, Y. C. Ding, M. Zhang, and Y. P. Tang, "Preparation and electroactive properties of a PVDF/nano-TiO<sub>2</sub> composite film," *Appl. Surf. Sci.*, Vol. 257, No. 9, pp. 3831-3835, Feb 15, 2011.
- [23] T. U. Patro, M. V. Mhalgi, D. V. Khakhar, and A. Misra, "Studies on poly(vinylidene fluoride)-clay nanocomposites: Effect of different clay modifiers," *Polymer*, Vol. 49, No. 16, pp. 3486-3499, 2008.
- [24] G. W. Ho, A. S. W. Wong, D.-J. Kang, and M. E. Welland, "Three-dimensional crystalline SiC nanowire flowers," *Nanotechnology*, Vol. 15, No. 8, pp. 996-999, 2004.
- [25] J. Sheth, D. Kumar, V. K. Tiwari, and P. Maiti, "Silicon carbide-induced piezoelectric beta-phase in poly(vinylidene fluoride) and its properties," *J. Mater. Res.*, Vol. 27, No. 14, pp. 1838-1845, Jul, 2012.
- [26] R. Gregorio, "Determination of the alpha, beta, and gamma crystalline phases of poly(vinylidene fluoride) films prepared at different conditions," *J. Appl. Polym. Sci.*, Vol. 100, No. 4, pp. 3272-3279, May 15, 2006.
- [27] D. M. Esterly, and B. J. Love, "Phase transformation to beta-poly(vinylidene fluoride) by milling," *J. Polym. Sci. Pol. Phys.*, Vol. 42, No. 1, pp. 91-97, Jan 1, 2004.
- [28] J. S. Lee, A. A. Prabu, and K. J. Kim, "Annealing effect upon chain orientation, crystalline morphology, and polarizability of ultra-thin P(VDF-TrFE) film for nonvolatile polymer memory device," *Polymer*, Vol. 51, No. 26, pp. 6319-6333, Dec 10, 2010.
- [29] D. Mandal, S. Yoon, and K. J. Kim, "Origin of Piezoelectricity in an Electrospun Poly(vinylidene fluoride-trifluoroethylene) Nanofiber Web-Based Nanogenerator and Nano-Pressure Sensor," *Macromol. Rapid Comm.*, Vol. 32, No. 11, pp. 831-837, Jun 1, 2011.
- [30] K. Tashiro, and M. Hanesaka, "Confirmation of crystal structure of poly(vinylidene fluoride) through the detailed structure analysis of vinylidene fluoride oligomers separated by supercritical fluid chromatography," *Macromolecules*, Vol. 75, No. 3, pp. 714-721, 2002.
- [31] T. C. Hsu, and P. H. Geil, "Deformation and transformation mechanisms of poly(vinylidene fluoride)(PVF<sub>2</sub>)," *J. Mater. Sci.*, Vol. 24, No. 4, pp. 1219-1232, 1989.
- [32] D. Mandal, K. J. Kim, and J. S. Lee, "Simple synthesis of palladium nanoparticles, beta-phase formation, and the control of chain and dipole orientations in palladium-doped poly(vinylidene fluoride) thin films," *Langmuir*, Vol. 28, No. 28, pp. 10310-7, Jul 17, 2012.
- [33] Y. C. Li, and S. C. Tjong, "Structure and Electrical Characteristics of Poly(vinylidene fluoride) Filled with Beta Silicon Carbide Nanoparticles," *J. Nanosci. and Nanotechnol.*, Vol. 11, No. 6, pp. 5148-5153, Jun, 2011.
- [34] F. Liu, R. Huo, X. Huang, Q. Lei, and P. Jiang, "Crystalline properties, dielectric response and thermal stability of in-situ reduced graphene oxide/poly(vinylidene fluoride) nanocomposites," *IEEE Trans. Dielectri. Electr. Insul.*, Vol. 21, No. 4, pp. 1446-1454, 2014.
- [35] G. Teyssedre, A. Bernes, and C. Lacabanne, "Influence of the crystalline phase on the molecular mobility of PVDF," *J. Polym. Sci. Pol. Phys.*, Vol. 31, No. 13, pp. 2027-2034, 1993.
- [36] S. Novak, J. Kovač, G. Dražić, J. M. F. Ferreira, and S. Quaresma, "Surface characterisation and modification of submicron and nanosized silicon carbide powders," *J. Eur. Ceram. Soc.*, Vol. 27, No. 12, pp. 3545-3550, 2007.
- [37] Q. Huang, P. Chen, M. Y. Gu, Y. P. Jin, and K. Sun, "Effect of surface modification on the rheological behavior of concentrated, aqueous SiC suspensions," *Mater. Lett.*, Vol. 56, No. 4, pp. 546-553, Oct, 2002.
- [38] D. S. Kim, H. B. Park, J. W. Rhim, and Y. M. Lee, "Proton conductivity and methanol transport behavior of cross-linked PVA/PAA/silica hybrid membranes," *Solid State Ionics*, Vol. 176, No. 1-2, pp. 117-126, Jan 14, 2005.
- [39] W. Wang, S. Zhang, L. O. Srisombat, T. R. Lee, and R. C. Advincula, "Gold-Nanoparticle- and Gold-Nanoshell- Induced Polymorphism in Poly(vinylidene fluoride)," *Macromol. Mater. Eng.*, Vol. 296, No. 2, pp. 178-184, 2011.

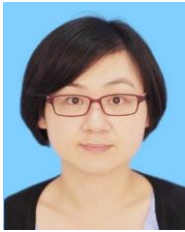


**Jie-Fang Huang** received the B.S. degree in Microelectronics from the School of Physics and Engineering, Sun Yat-Sen University, Guangzhou, China, in 2014. She has researched on self-powered electronics based on piezoelectricity and triboelectricity in the State Key Laboratory of Optoelectronic Materials and Technologies since 2013. Miss Huang is pursuing her master degree in the major of Microelectronics and Solid-State Electronics now, focusing on flexible and wearable

pressure sensor.



**Song-Jia Han** received the B.S. degree in school of materials science and engineering from Wuhan University of Technology, Wuhan, China, in 2010 and the M.S. degree in college of polymer science and engineering from Sichuan University, Chengdu, China, in 2013. Since 2013, she joined Sun Yat-Sen University, as a research assistant, researching on the development of the transparent conductive films and piezoelectric sensor.

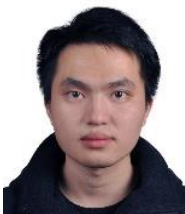


**Hui-Jiuan Chen** received the B.S. degree in clinical medicine from Fujian Medical University, Fuzhou, China, in 2006 and the M.S. degree in biomedical engineering from Queen Mary University of London, London, UK, in 2009 as well as the Ph.D. degree in material science at Queen Mary University of London, London, UK, in 2013. Since 2013, she has been an Associate Research Fellow with the SYSU-CMU Shunde International Joint Research Institute. She has published more than 10 articles. Her

research interest includes applying nanoparticles in the biomedical direction, covering a wide spectrum of nanotechnology, medicine and engineering science, centered on preparations and applications of nanomaterials, such as, flexible device, various thermal therapies. Dr. Chen's award includes Third Prize for the Best Oral Presentation, 17th CSCST-SCI conference, 2011.



**Gui-Shi Liu** received the B.S. degree in applied physics from the East China Institute of Technology, Nanchang, China, in 2008 and the M.S. degree in plasma physics from Dalian University of Technology, Dalian, China, in 2011. He is currently working toward the Ph.D. degree in microelectronics and solid state electronics at Sun Yat-Sen University, Guangzhou, China. His research interests include patterning, transfer printing of silver nanowires for sensors.



**Gong-Tan Li** received his B.S. degree in material physics from the School of Physics and Engineering, Sun Yat-Sen University, Guangzhou, China, in 2011. Since Sep. 2011, he was working for Ph. D degree in the major of the microelectronics, researching on oxide thin film transistors in the State Key Laboratory of Optoelectronic Materials and Technologies.



**Yu-Cheng Wang** received the B.S. degree in Information Display & Optoelectronics technology from the School of Physics and Engineering, Sun Yat-Sen University, Guangzhou, China, in 2015. He is now a graduate student in the major of Microelectronics and

Solid-State Electronics, researching on e-paper display and self-power electronics in the State Key Laboratory of Optoelectronic Materials and Technologies.



**Zi-Xin Wang** received his B.Sc. degree in Physics, M.S. and Ph.D. degrees in Optical engineering from Sun Yat-Sen University, in 1999, 2002, and 2006, respectively. In 2006, he joined the Department of Microelectronics at Sun Yat-Sen University, as an assistant professor. His specific research interests are low noise electronic techniques, lock-in amplification system, mixed-signal and high level synthesis. He is currently an associate professor.



**Bo-Ru (Paul) Yang** received his B.S. and M.S. degrees in Department of Material Science and Engineering from National Chiao Tung University (NCTU), Taiwan, in 2002 and National Tsing Hua University, Taiwan, in 2004, respectively. In 2008, he received his Ph.D. in Institute of Electro-Optical Engineering from NCTU, Taiwan, where he also finished an MBA program simultaneously. During his time studying Ph.D., he received the scholarships to study fast-switching LCD at University of Oxford, UK in 2007 and Tohoku University, JP in 2008 as a doctoral researcher. He was working with SiPix-Eink during 2009-2012. Since Dec. 2012, he joined Sun Yat-Sen University, China, as an associate professor, researching on the flexible electronics and displays. He is also an associate editor of Journal of Society for Information Display, JSID, and vice chair of flexible display and E-paper committee in SID 2017.



**Zhen-Hua Luo** received the B.Sc. degree in Nanotechnology in 2006, and the Ph.D. degree in 2011 from the University of New South Wales, Australia. His Ph.D. research was studying the PZT and lead-free piezoelectric ceramics. In 2009 he was working as a visiting researcher in the Technical University of Darmstadt, Germany, to research the lead-free piezoelectric ceramics including BNT-BT and KNN. In 2012 and 2013 he worked as a R&D manager in a LED manufacturing company to develop energy harvesting floor. He joined the University of Southampton, UK, in 2013, currently working as a research fellow in EPSRC funded SPHERE project to develop energy harvesting solutions for residential sensing environment. His research interests include piezoelectric and solar energy harvesting, advanced piezoelectric materials and nanofabrication.



**Han-Ping D. Shieh** received the B.S. degree from National Taiwan University in 1975 and Ph.D. in electrical and computer engineering from Carnegie Mellon University, Pittsburgh, PA, U.S.A. in 1987. He joined National Chiao Tung University (NCTU) in Hsinchu, Taiwan as a professor at Institute of Opto-Electronic Engineering and Microelectronics and Information Research Center (MIRC) in 1992 after as a Research Staff Member at IBM TJ Watson Research Center, Yorktown Heights, NY, USA since 1988. He founded and served as the Director, Display Institute at NCTU in 2003, the first such kind of graduate academic institute in the world dedicated for display education and research. He was the Dean, College of Electrical and Computer Engineering, NCTU (2006–2010) and AU Optronics Chair Professor. He is now an NCTU Chair Professor and a NCTU senior vice President. He is also holding an appointment as a Chang Jiang Scholar at Shanghai Jiao Tong University since 2010. Dr. Shieh is a fellow of IEEE, OSA and SID (Society for Information Display).